

Photoproduction of mesons from nuclei - In-medium properties of hadrons

B. Krusche,¹

¹Department of Physics and Astronomy, University of Basel, Switzerland

November 5, 2018

Abstract

Recent experimental results for the in-medium properties of hadrons obtained with photoproduction of mesons from nuclei are discussed. The experiments were done with the TAPS detector at the tagged photon beam of the MAMI accelerator in Mainz. Measured were the final states $\pi^o X$, ηX , $2\pi^o X$, and $\pi^o \pi^\pm X$ for ^{12}C , ^{40}Ca , ^{93}Nb , and ^{208}Pb up to the second resonance region. The results were used for an investigation of the in-medium properties of the $P_{33}(1232)$, the $P_{11}(1440)$, the $D_{13}(1520)$, and the $S_{11}(1535)$ resonances. It was found that the cross sections can be split into a component which originates from the low density surface region of the nuclei and a component which scales like the nuclear volume. The energy dependence of the surface component is strikingly similar to the deuteron, it shows a clear signal for the second resonance peak. The volume component is lacking this peak and shows an enhancement at intermediate energies. Furthermore the measurement of coherent η -photoproduction and the final state $p\pi^o$ from ^3He is discussed in the context of the search for η -mesic nuclei.

1 Introduction

In-medium properties of hadrons are a hotly debated topic since they are closely connected to the properties of low energy non-perturbative QCD. QCD at high energies or short scales ($r < 0.1$ fm) is a perturbative theory with point-like quarks and gluons. However, at larger distances the perturbative picture breaks down. In the intermediate range ($0.1 \text{ fm} < r < 1 \text{ fm}$) the physics is governed by the excitation of nucleon resonances. This is the regime where the full complexity of the structure of the nucleon as a many body system with valence quarks, sea quarks and gluons contributes. Apart from lattice gauge calculations, so far only models with effective degrees of freedom such as constituent quarks and flux tubes are applicable to this problem. At even larger distances beyond 1 fm, QCD becomes the theory of nucleons and mesons (pions) and can be treated in the framework of chiral perturbation theory. Chiral symmetry is at the very heart of low energy QCD. In the limit of vanishing current quark masses the chiral Lagrangian is invariant under chiral rotations, right- and left-handedness of quarks is conserved and right- and left-handed fields can be treated independently. The explicit breaking of chiral symmetry due to the finite u,d current quark masses (5-15 MeV) is small. However, it is well known, that chiral symmetry is spontaneously broken since the ground state, the QCD vacuum, has only part of the symmetry of the Lagrangian. This is connected with a non-zero expectation value of scalar $q\bar{q}$ pairs in the vacuum, the so-called chiral condensate. A consequence of the chiral symmetry breaking in

the hadron spectra is the non-degeneracy of parity doublets. The $J^\pi = 0^-$ pion (the Goldstone boson of chiral symmetry) is much lighter than its chiral partner the $J^\pi = 0^+$ σ meson. Similarly, the lowest lying $J^\pi = 1^-$ meson, the ρ has a smaller mass than the $J^\pi = 1^+$ a_1 and also the first $J^\pi = 1/2^-$ excited state in the baryon spectrum, the $S_{11}(1535)$, lies much above the $J^\pi = 1/2^+$ nucleon ground state.

Model calculations indicate a significant temperature and density dependence of the chiral condensate (see e.g. [1]). This behavior is illustrated in fig. 1. The melting of the chiral condensate is connected with a predicted partial restoration of chiral symmetry at high temperatures and/or large densities. The different regimes are in particular accessible in heavy ion reactions, but the effect is already significant at zero temperature and normal nuclear matter density, i.e. conditions which can be probed with photon and pion beams. One consequence of the partial chiral symmetry restoration is a density dependence of hadron masses. An early prediction for this effect is the so-called Brown-Rho scaling [2]:

$$m_{\sigma,\rho,\omega}^*/m_{\sigma,\rho,\omega} \approx m_N^*/m_N \approx f_\pi^*/f_\pi, \quad (1)$$

where m^* are the in-medium masses and f_π is the pion decay constant. Simple approximations of the mass dependence, for example in the framework of the linear sigma model, parameterize it linearly in the nuclear density [3]:

$$m_{\sigma,\rho}^* \approx m_{\sigma,\rho} \left(1 - \alpha_{\sigma,\rho} \frac{\rho}{\rho_0} \right) \quad (2)$$

with α in the range 0.2 - 0.3. Evidence for such effects has been searched for in many experiments. An example is the search for the predicted shift and broadening of the ρ -meson in the di-lepton spectra of heavy ion reactions with CERES at CERN [4, 5] and in the near future with the HADES detector at GSI. Heavy ion induced reactions profit from the relatively large densities reached in the collision phase, but suffer from the complicated interpretation of the rapidly varying, highly non-equilibrium reaction conditions. More recently, also pion and photon induced reactions on nuclei, which test the hadron properties at normal nuclear matter density, have moved into the focus. A much discussed effect in this field is the in-medium modification of the σ meson, respectively the modification of the $\pi\pi$ interaction in the scalar - isoscalar channel, reported from the CHAOS [6] and Crystal Ball collaborations [7] for pion induced double pion production.

In-medium modifications of mesons will of course also influence the in-medium properties of nucleon resonances due to the coupling between resonances and mesons. Recently, Post, Leupold and Mosel [8] have calculated in a self consistent way the spectral functions of mesons and baryons in nuclear matter from these couplings. The most relevant contributions to the self-energies are shown in fig. 2. In the vacuum mesons like the ρ can couple only to meson loops (involving e.g. the pion) and nucleon resonances couple to nucleon - meson loops. However, in the medium mesons can couple to resonance - hole states (the best known example is the coupling of the pion to $\Delta - h$ states in Δ - hole models). This influences not only the spectral functions of the mesons, but also the resonances which in turn couple to the modified meson loops. It makes necessary an iterative, self-consistent treatment of the self-energies. The predicted effects are in particular large for the ρ meson and the $D_{13}(1520)$ resonance due to the strong coupling of the resonance to $N\rho$. The close by $S_{11}(1535)$ resonance is much less effected (see [8]).

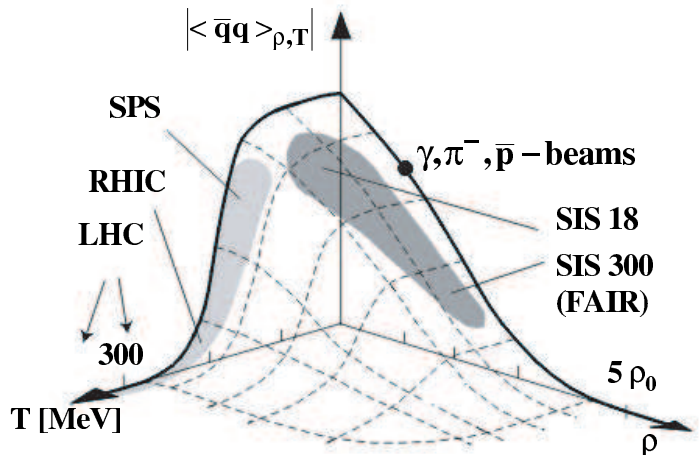


Figure 1: Chiral condensate as function of temperature T and nuclear density ρ (ρ_0 normal nuclear matter density)

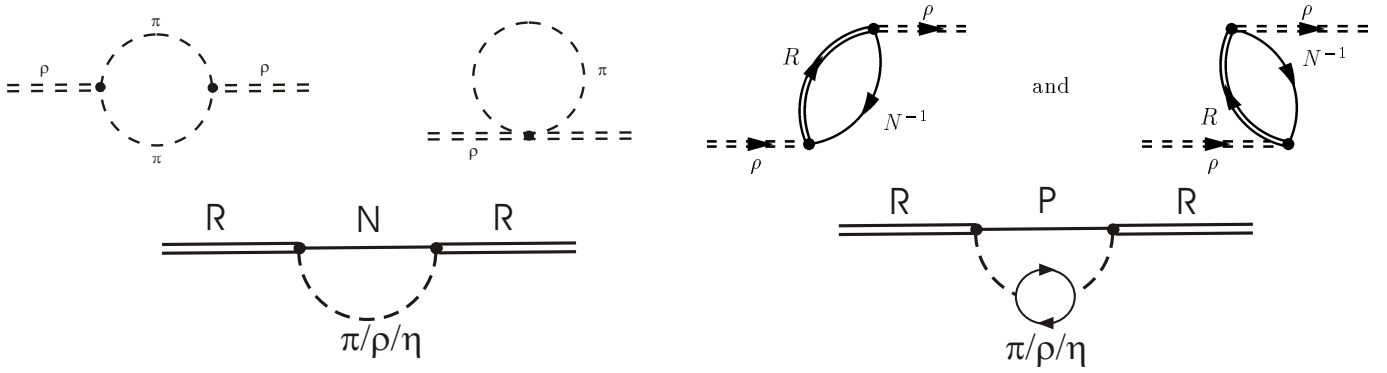


Figure 2: Self energies from coupling of mesons and nucleon resonances, left hand side: vacuum, right hand side: in the nuclear medium [8]

During the last few years, the TAPS collaboration has engaged in a program to study the in-medium properties of mesons and nucleon resonances and the meson - nucleus interactions with photon induced meson production reactions from nuclei. This program covers four different major topics:

- The investigation of resonance contributions to η , π , 2π meson production reactions from nuclei aiming at resonance in-medium properties like mass and width [9, 11]
- The search for η - nucleus bound states (so-called η -mesic nuclei), which would be the ideal testing ground for the investigation of the η - nucleus interaction [12]
- The investigation of the pion - pion invariant mass distributions for $2\pi^0$ and $\pi^0\pi^\pm$ production from nuclei, aiming at the in-medium behavior of the ' σ '-meson [13]
- The measurement of the resonance shape of the ω meson in nuclear matter from its $\pi^0\gamma$ decay

The first two topics will be discussed in this contribution, the status of the other two topics is summarized by V. Metag in the proceedings to the same conference.

2 Experiments

The experiments discussed in this contribution were carried out at the Glasgow tagged photon facility installed at the Mainz microtron MAMI. The experiments used Bremsstrahlung photons produced with the 850 MeV electron beam in a radiator foil. The standard tagging range covers photon energies between 50 and 790 MeV, although for many experiments the low energy section of the tagger is switched off, to allow for higher intensities at high photon energies. This is possible since the electron beam intensity is limited by the fastest counting photomultipliers in the tagger focal plane at intensities far below the capabilities of the electron machine. The maximum tagged photon energies were 820 MeV with a typical focal plane energy resolution of 2 MeV. However, since the intrinsic resolution of the magnet is much better (roughly 100 keV), the use of 'tagger microscopes' with scintillation counters of much smaller width is possible and planned for example for the second generation experiments searching for η -mesic nuclei.

The meson production experiments were carried out with the electromagnetic calorimeter TAPS [14, 15]. The setup is shown in fig. 3. It consists of more than 500 hexagonally shaped BaF_2 scintillators of 25 cm length corresponding to 12 radiation lengths. The device is optimized for the detection of photons, but has also particle detection capabilities. The separation of photons from massive particles makes use of the plastic veto detectors (only charged particles), a time-of-flight measurement with

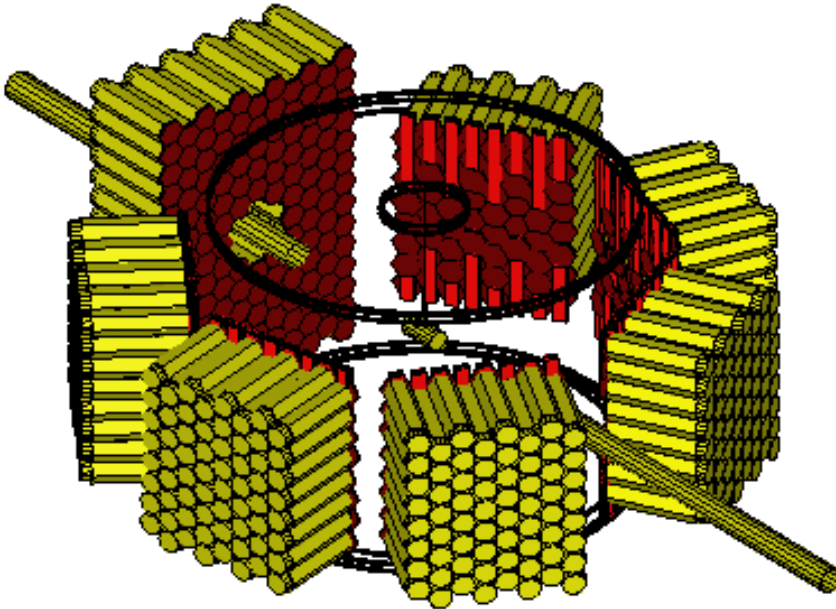


Figure 3: Setup of the TAPS detector at the Mainz MAMI accelerator. Six block structures with 64 BaF_2 modules each and one forward wall with 120 crystals were arranged in one plane around the target. The detector modules are equipped with individual plastic veto detectors for charged particle discrimination. The beam enters from the lower right corner.

typically 500 ps resolution (FWHM) and the excellent pulse shape discrimination capabilities of BaF_2 -scintillators. The combination of these methods produces extremely clean samples of the meson decay photons. The identification of neutral mesons (π^0 and η) then makes use of a standard invariant mass analysis. Charged mesons and nucleons are identified in addition with time-of-flight versus energy analyses. Details of the analysis procedures and the identification of different reaction channels are summarized in [10, 11].

3 Results

Data have been taken for ^2H , $^3,4\text{He}$, ^{12}C , ^{40}Ca , ^{93}Nb and ^{208}Pb targets (the carbon, calcium and lead targets were not isotopic pure). The data from the deuteron were used as a reference point for the elementary cross sections from the quasifree nucleon. Compared to the free proton this has the advantage that it automatically averages over neutron and proton cross section. The measurement with the helium targets were motivated by the detailed investigation of η threshold production from light nuclei in view of the η - nucleus interaction.

3.1 The $\Delta(1232)$ resonance

The excitation of the Δ resonance and its propagation through the nuclear medium have been intensively studied in heavy ion reactions [23], in pion, electron, and photon induced reactions [24, 25]. An in-medium broadening at normal nuclear matter density of roughly 100 MeV has been extracted from pion nucleus scattering experiments [26]. A detailed understanding of the in-medium properties of this state is necessary for any interpretation of pion photoproduction reactions from nuclei. It dominates single pion production in the low energy region up to 500 MeV incident photon energies, but it also contributes at higher energies via multiple pion production processes and through re-absorption of pions. In photon induced reactions on the free proton, single π^0 photoproduction is best suited to study this state. This is demonstrated in fig. 4, with a comparison of the total cross sections for neutral and charged pion production from the proton. The background from non-resonant contributions is much more pronounced in the charged channel where pion-pole and Kroll-Rudermann terms contribute. Such contributions are suppressed for neutral pions so that $\gamma p \rightarrow p\pi^0$ is dominated by the Δ already close to threshold. However, for nuclei a further complication arises. Neutral pions can be produced in two

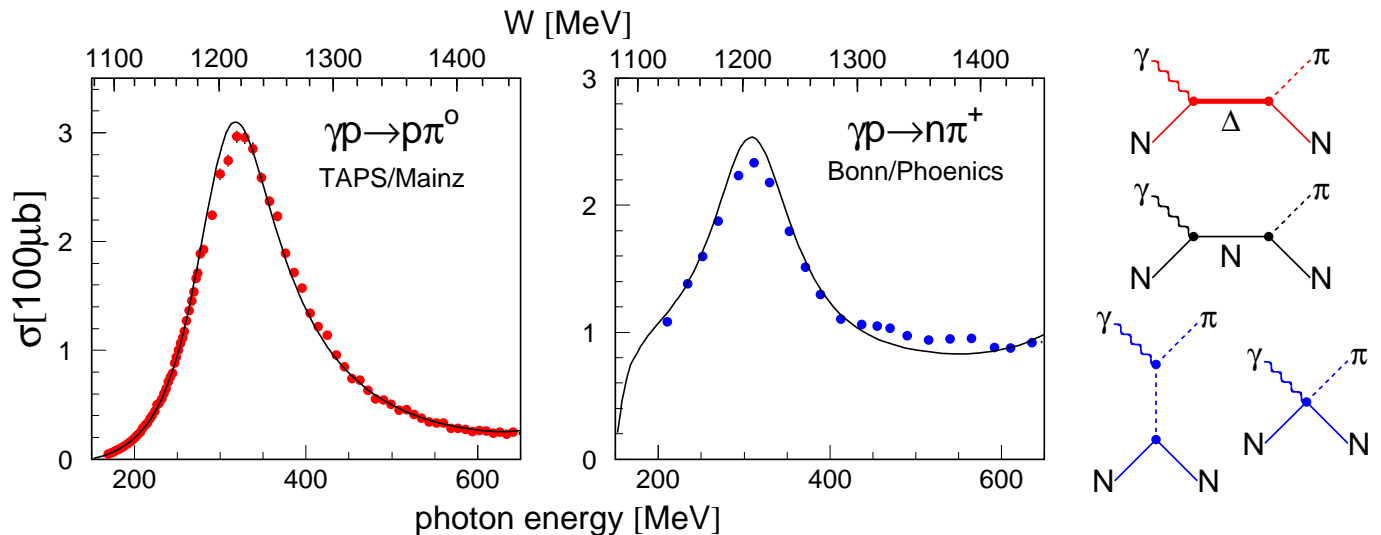


Figure 4: Total cross sections for pion photoproduction from the proton in the Δ -resonance region. Data from [16, 10] ($p\pi^0$) and [17] ($n\pi^+$). Curves from MAID2000 [18].

different reaction types with very different characteristics. In (quasifree) breakup reactions in simplest plane wave approximation the pion is produced from a single nucleon which in the process is knocked out of the nucleus. As long as the momentum transfer is not too high, this process competes with coherent π^0 production. In this case the amplitudes from all nucleons add coherently, the momentum transfer is taken by the entire nucleus, and no nucleons are removed. The two reaction mechanisms can be separated via their different kinematics. The total cross sections for the deuteron and the heavy nuclei are summarized for both reaction mechanisms [10, 20, 11] in fig. 5. Their behavior is quite

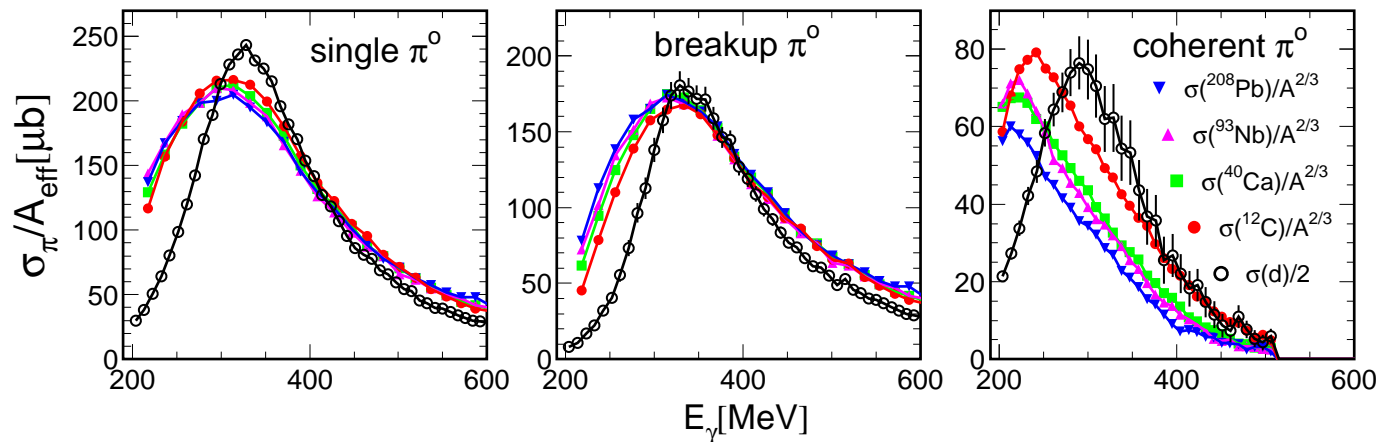


Figure 5: Total cross sections for π^0 production in the Δ resonance from the deuteron and from heavy nuclei. Left hand side: coherent part, middle: breakup part, right hand side: sum of both [10, 20, 11]. The legend is valid for all three pictures.

different. The coherent reaction can be approximated for spin $J = 0$ nuclei in plane wave by:

$$\frac{d\sigma_A}{d\Omega} \propto \frac{d\sigma_N}{d\Omega} A^2 F^2(q) \sin^2(\Theta^*) \quad (3)$$

where $d\sigma_A$ is the nuclear cross section, $d\sigma_N$ the elementary cross section on the free nucleon, A the atomic mass number, $F^2(q)$ the nuclear form factor depending on the momentum transfer q , and Θ^* the cm polar angle of the pion (for details see [20]). The observed shift of the peak cross section to low

photon energies for heavy nuclei is not related to in-medium effects of the Δ but is a simple consequence of the interplay between the $F^2(q)$ and $\sin^2(\Theta^*)$ factors. An extraction of Δ in-medium properties from the coherent cross section requires more detailed DWIA calculations (see below).

It is tempting to argue, that the breakup process, where the pion is produced in quasifree kinematics from an individual nucleon, is best suited to study the Δ in-medium line-shape. However, quasifree and coherent contributions are not independent. They are closely connected via final state interaction (FSI), which was discussed in detail for the deuteron in [10, 27]. Siodlaczek et al. [27] have even argued that for the deuteron the effect of FSI in the breakup process is just counterbalanced by the coherent process so that the sum of the cross sections for the coherent and the breakup part with FSI equals the cross section of the pure quasifree process without FSI. As shown in fig. 6 a similar effect is also visible

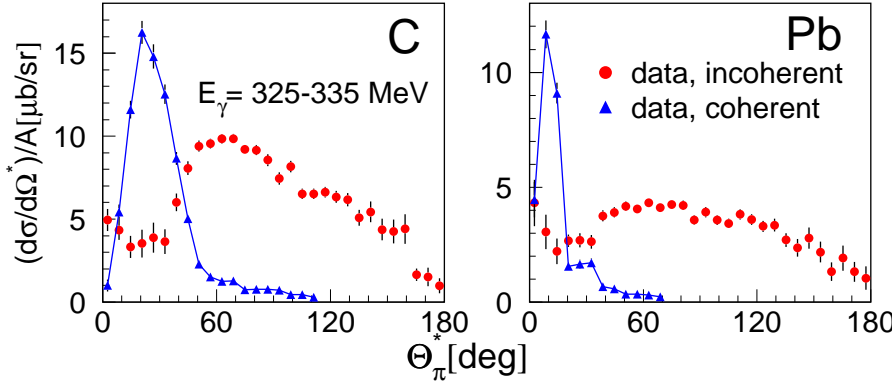


Figure 6: Angular distributions for breakup and coherent π^0 photoproduction from carbon and lead [11].

in the angular distributions of single pion photoproduction from heavy nuclei [11]. The breakup cross section is depleted at forward angles where the coherent cross section peaks. Forward angles of the pion correspond to backward angles of the struck nucleon, i.e. to small nucleon momenta which may lead to Pauli-blocked nucleon final states. The cross section for inclusive single π^0 photoproduction, i.e. the sum of breakup and quasifree parts can thus serve as a first approximation. It scales almost perfectly with $A^{2/3}$, which of course indicates strong FSI effects. The average over the heavy nuclei is compared in fig. 7 to the cross section from the free proton. The Δ -resonance peak for the nuclei is

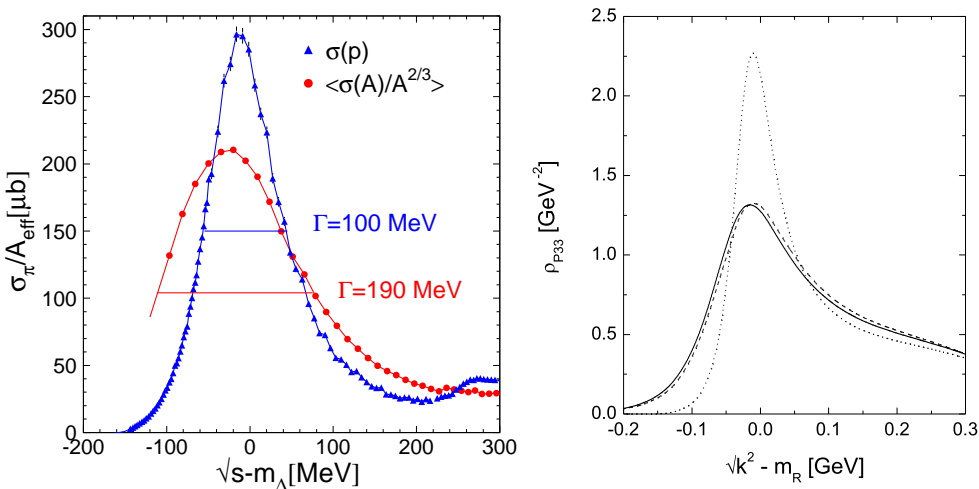


Figure 7: Left hand side: total π^0 photoproduction from the proton compared to the average for heavy nuclei. Right hand side: self consistent spectral functions for the Δ resonance in vacuum and in the nuclear medium [8].

significantly broadened with respect to the free nucleon from 100 MeV to 190 MeV (note that nuclear Fermi motion causes only a much smaller broadening). This is in nice agreement with the prediction for the in-medium spectral function of the Δ [8](see fig. 7, right hand side), which corresponds to exactly the same broadening.

A more detailed separate analysis of the breakup and coherent components requires models. The breakup process is mostly treated in the framework of nuclear cascade models or transport models.

The data are compared in fig. 8 to calculations in the framework of the Boltzmann-Uehling-Uhlenbeck transport model [19, 11]. The model includes an additional in-medium width of the Δ of roughly 80 MeV at normal nuclear matter density. The calculations reproduce the shift of the rising slope of the

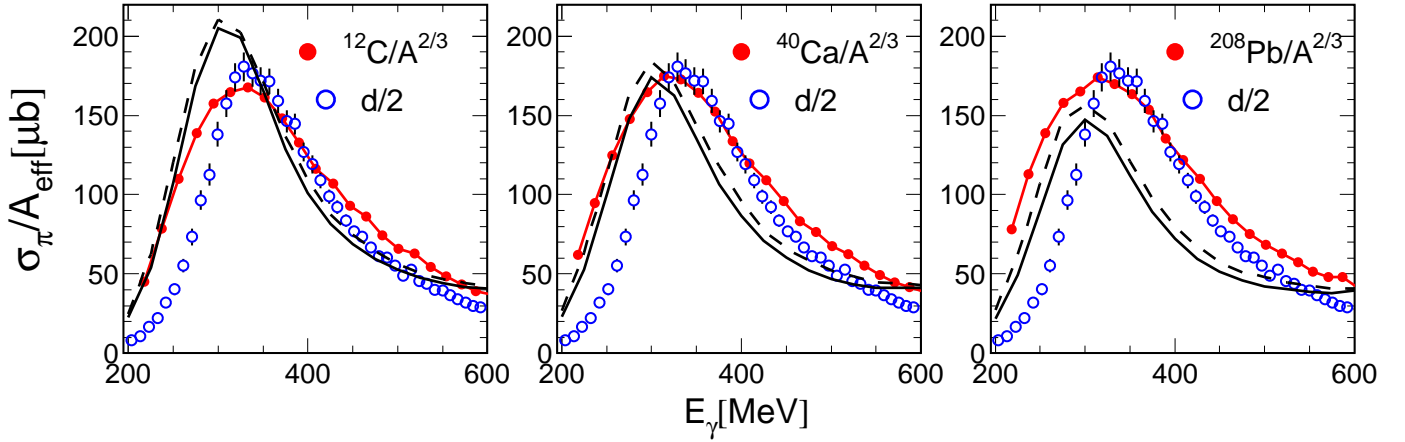


Figure 8: Quasifree photoproduction of single π^0 mesons from the deuteron and from heavy nuclei compared to BUU-model calculations [19, 11] for heavy nuclei. The different curves correspond to slightly different parameterizations of the Δ in-medium width.

Δ to lower incident photon energies, but underestimate the falling slope and show a somewhat different mass number dependence of the peak cross section. Note however, that for a heavy nucleus like lead FSI reduces the peak cross section by more than a factor of four, so that the result is extremely sensitive to the details of FSI in the model. The problems in the high energy tail of the Δ may be partly attributed to two-body absorption processes of the photon which are not included in the model.

The results from coherent π^0 photoproduction from nuclei have been analyzed in detail in [28, 20] in the framework of the DWIA calculations of Drechsel, Tiator, Kamalov and Yang [21] which include a phenomenological Δ self-energy. The result for the total cross section is shown in fig. 9. The main

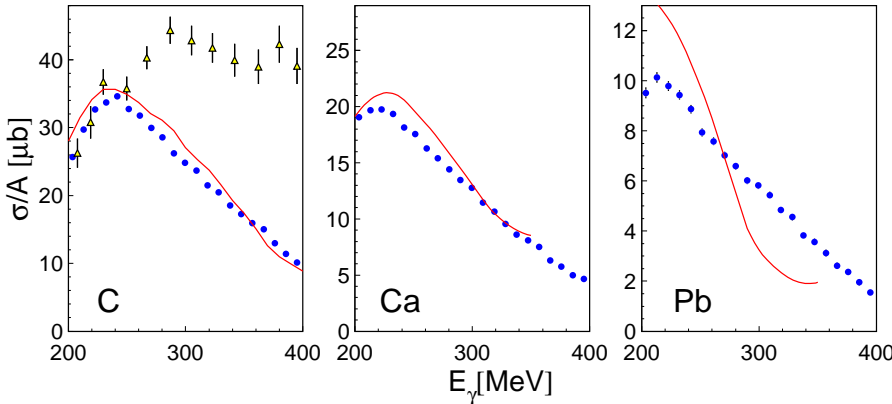


Figure 9: Total cross sections for coherent π^0 photoproduction from nuclei [20]. The curves are calculations from [21]. The triangles for ^{12}C are from a previous measurement with less stringent suppression of the incoherent components [22].

finding was, that the model with the self-energy fitted to ^4He reproduces the data for carbon and calcium almost perfectly so that no significant mass dependence of the self-energy was found. The self-energy itself corresponds to an increase of the width at resonance position ($E_\gamma \approx 330$ MeV) of roughly 110 MeV in agreement with the results discussed above. The resonance position is slightly upward shifted (by 20 MeV). This is no contradiction to the excitation functions in fig. 7. The width increase is energy dependent (only ≈ 40 MeV at $E_\gamma \approx 250$ MeV) so that the net effect in the excitation functions in fig. 7 is a small downward shift of the peak position.

3.2 The second resonance region

Among the clearest experimental observations of in-medium effects is the suppression of the second resonance peak in total photoabsorption (TPA) experiments [29, 30, 31]. TPA on the free proton shows a peak-like structure at incident photon energies between 600 and 800 MeV, which is attributed to the excitation of the $P_{11}(1440)$, $D_{13}(1520)$, and $S_{11}(1535)$ resonances. This structure is not visible for nuclei over a wide range of mass numbers from lithium to uranium (see fig. 10, left hand side). A

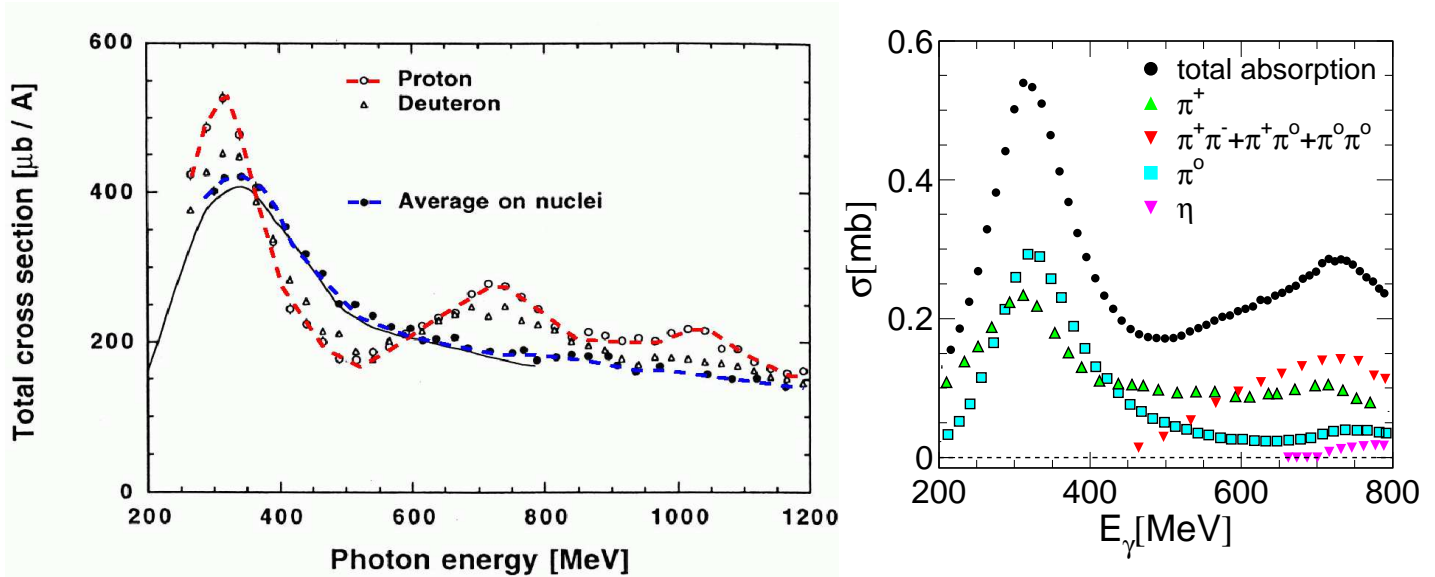


Figure 10: Left hand side: total photoabsorption from the proton, the deuteron and the average for heavy nuclei [31]. Right hand side: Partial cross sections for photoproduction from the proton [10, 17, 32, 33, 34, 35, 36].

broadening due to nuclear Fermi motion certainly contributes, but cannot explain the full effect. Some authors [42, 43] have argued for an in-medium width of the relevant nucleon resonances, in particular the $D_{13}(1520)$, on the order of 300 MeV. Such an assumption brings model predictions close to the data but it is not clear which effect should be responsible for such a large broadening. Post, Leupold and Mosel [8] find in their coupled channel analysis of in-medium spectral functions of mesons and resonances a relatively strong broadening of the D_{13} and a much smaller effect for the S_{11} . Possible effects resulting from the collisional broadening of the resonances have been studied in detail in the framework of transport models of the BUU-type (see e.g. [19]), but up to now the complete disappearance of the resonance structure was not explained.

The resonance bump on the free proton consists of a superposition of reaction channels with different energy dependencies (see fig. 10, right hand side) which complicates the situation [46]. Much of the rise of the cross section towards the maximum around 750 MeV is due to the double pion decay channels, in particular to the $n\pi^0\pi^+$ and $p\pi^+\pi^-$ final states. Gomez Tejedor and Oset [44] have pointed out that for the latter the peaking of the cross section is related to an interference between the leading Δ -Kroll-Rudermann term and the sequential decay of the D_{13} resonance via $D_{13} \rightarrow \Delta\pi$. Hirata et al. [45] have argued that the change of this interference effect in the nuclear medium is one of the most important reasons for the suppression of the bump.

Inclusive reactions like total photoabsorption alone do not allow a detailed investigation of such effects. A study of the partial reaction channels is desirable. The experimental identification of exclusive final states is more involved and FSI effects must be accounted for. The interpretation of exclusive measurements therefore always needs models which account for the trivial in-medium and FSI effects like absorption of mesons and propagation of mesons and resonances through nuclear matter. On

the other hand, as a by-product, the analysis of the FSI effects enables the study of meson-nucleus interactions.

The results for meson photoproduction off the free proton suggest, that pion and η photoproduction are best suited for a comparison of the in-medium properties of the D_{13} and S_{11} resonances [46]. This is demonstrated in fig. 11 where the measured cross sections are compared to the results of the MAID model. The total cross section for η photoproduction is completely dominated in the second resonance

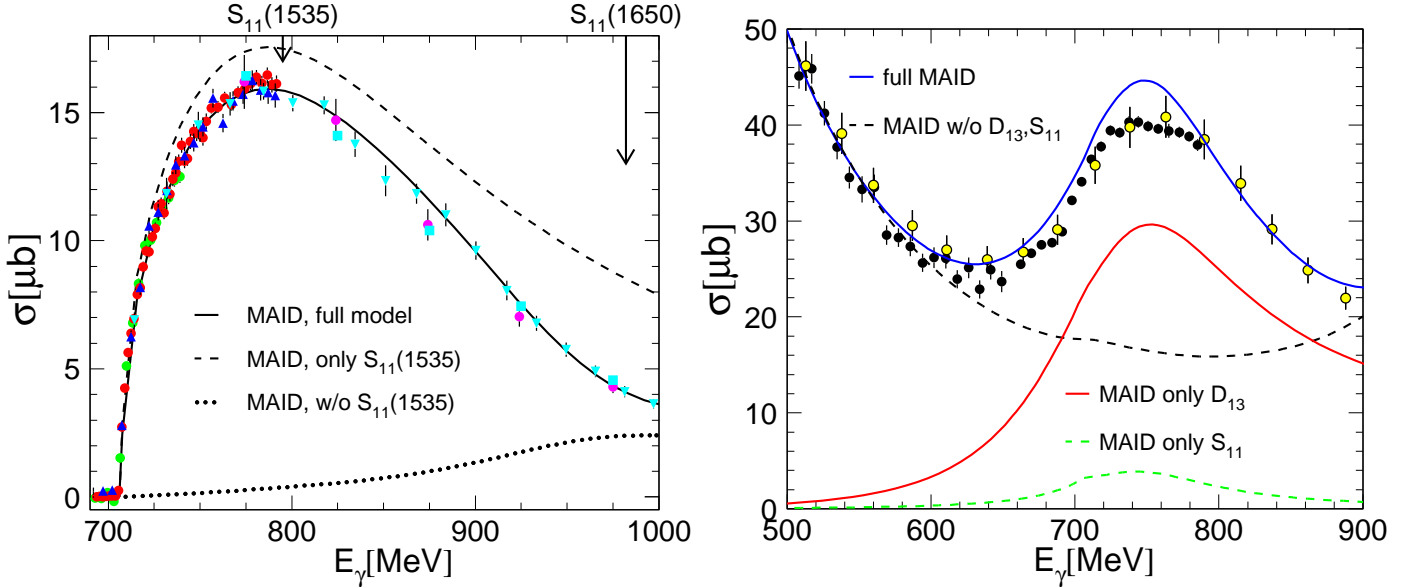


Figure 11: Resonance contributions to meson photoproduction off the proton in the second resonance region. Left hand side: η and the $S_{11}(1535)$. Data from [33, 37, 38, 39], curves from the ETA-MAID model [40]. Right hand side: π^0 and the $D_{13}(1520)$. Data from [10, 41] curves from MAID [18].

region by the $S_{11}(1535)$ resonance [47]. The D_{13} has no influence on the total cross section and only at higher incident photon energies the second S_{11} plays a significant role. On the other hand, the resonance structure in π^0 photoproduction is strongly dominated by the $D_{13}(1520)$ resonance.

Photoproduction of η mesons from light to heavy nuclei has been measured with TAPS at MAMI [9] up to incident photon energies of 800 MeV and at KEK in Japan up to 1 GeV [50, 51]. A comparison of the low energy data for the deuteron, ^{12}C , ^{40}Ca , ^{93}Nb and ^{208}Pb shows a perfect scaling with $A^{2/3}$ (the small deviation for the deuteron close to threshold is due to the smaller Fermi momenta), which indicates strong FSI. A comparison to calculations with the BUU model [19] or a mean free path Monte Carlo model [54] did not reveal any in-medium effects for the width or position of the resonance nor any depletion of its excitation strength [9]. A certain drawback of these data is certainly that they cover the S_{11} resonance only up to its maximum. The KEK measurements extend somewhat beyond the resonance position into the downward slope of the excitation functions. The authors claim from a comparison of the data to quantum Monte Carlo calculations some evidence for a broadening of the resonance structure with respect to the elementary reaction on the free proton. Statistically more precise data over an even much larger energy range (beyond 2 GeV) have been recently measured with TAPS and the Crystal Barrel at the Bonn ELSA accelerator. These data are still under analysis. However, the preliminary results indicate relatively large background contributions from $\pi\eta$ final states at incident photon energies beyond 900 MeV, which have to be suppressed by cuts on the reaction kinematics. This effect may have contributed to the observed broadening of the resonance structure in the KEK data, where no kinematical cuts were applied. In any way, the claimed in-medium effects for the S_{11} are not large. A comparison of the data to recent BUU calculations [52] is shown in fig. 12 right hand side. The main result is, that the data are better described when the momentum dependence of the in-medium

potential for nucleons and the S_{11} is included, but in agreement with the predicted in-medium spectral function of the S_{11} [8] only small collisional broadening effects are consistent with the data.

The predicted effects for the D_{13} resonance are much larger due to its strong coupling to the ρ meson [8]. Excitation functions for single π^0 photoproduction from the proton, the deuteron and off heavy nuclei are compared in fig. 13 [53]. Surprisingly, the resonance structure is not significantly broader for the heavy nuclei. Also the scaling with the mass number follows the general pattern (see below),

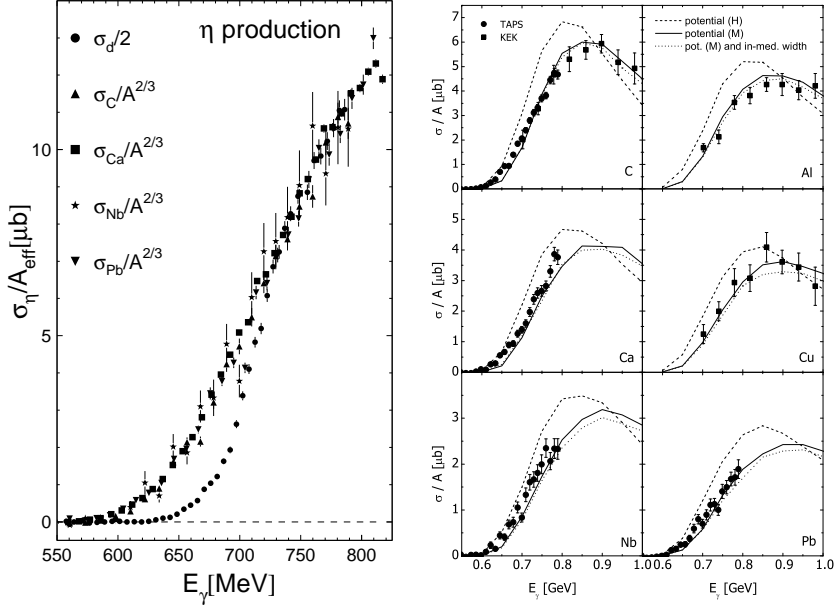


Figure 12: Total cross section for η photoproduction from nuclei. Left hand side: scaling of cross sections with mass number. Data from [9, 11, 48, 49]. Right hand side: comparison of data [9, 50, 51] to BUU calculations [52]. Dashed lines: momentum independent potentials, full lines: momentum dependent potentials, dotted: additional in-medium broadening of the S_{11}

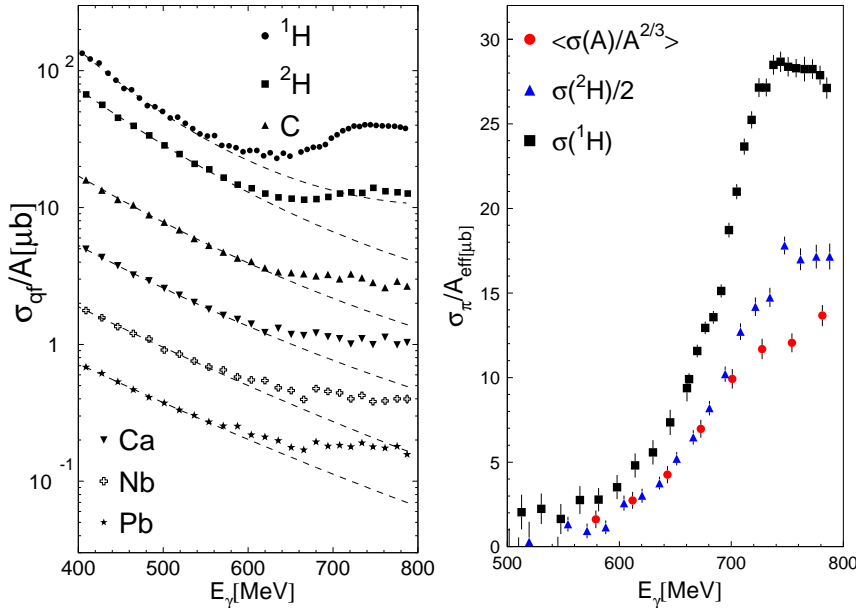


Figure 13: Total cross section for single π^0 photoproduction from nuclei [10, 53]. Left hand side: total cross section with fitted background (fit range 350 - 550 MeV). Scale corresponds to proton data, other data scaled down by factors 2,4,8,16, and 32. Right hand side: resonance signal with background subtracted. For the heavy nuclei only the average is shown.

apart from the fact that a fairly large reduction of the strength occurs for the deuteron with respect to the proton. This latter effect is also not yet understood [10], predictions for the cross section of $n(\gamma, \pi^0)n$ from multipole analyses of pion production are not in agreement with the observed deuteron cross section.

A possible explanation for the basically unchanged shape of the D_{13} observed in nuclear pion production could be, that due to FSI, only pions from the low density surface region are observed. The absorption properties of nuclear matter for pions as function of their momentum are summarized in fig.

14. The left hand side of the figure shows the ratio $R_{C2/3}$ of the cross sections for the heavier nuclei and carbon under the assumption of surface scaling:

$$R_{C2/3} \equiv \frac{[d\sigma/dp_\pi(A)]/A^{2/3}}{[d\sigma/dp_\pi(^{12}C)]/12^{2/3}} \quad (4)$$

The right hand side shows the scaling exponent α for a power law scaling $\propto A^\alpha$.

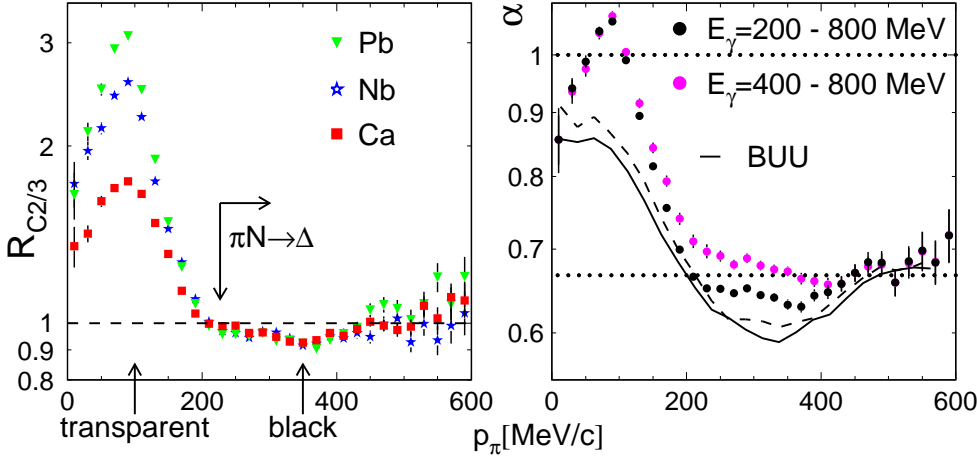


Figure 14: Scaling of π^0 cross sections as function of pion momentum. Left hand side: ratio $R_{C2/3}$. Right hand side: scaling coefficient α determined from $d\sigma/dp_\pi \propto A^\alpha$ [11]. Curves from BUU calculations with slightly different treatment of the Δ [19, 11].

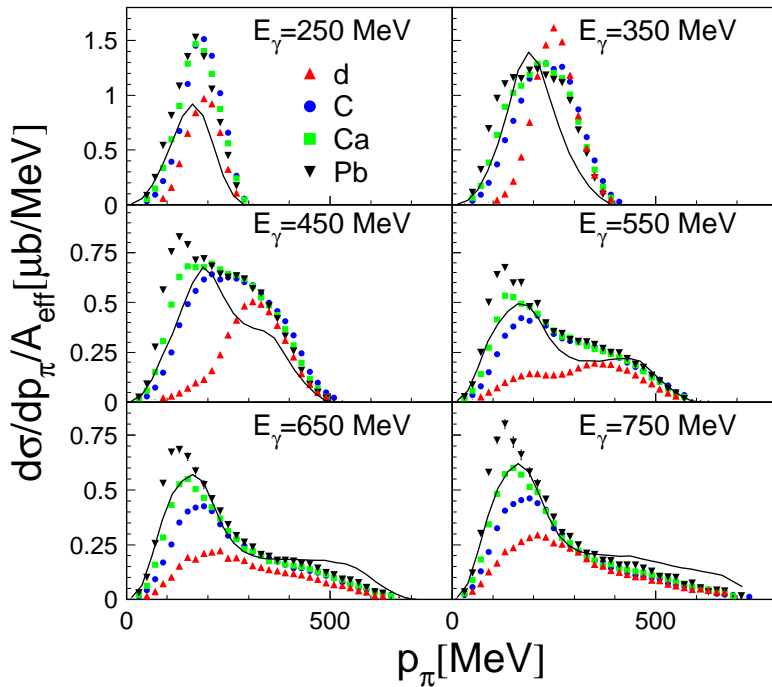


Figure 15: Momentum distributions for inclusive π^0 photoproduction from nuclei (scaled by $A_{eff} = A^{2/3}$ for $A > 2$ and by $A_{eff} = 2$ for the deuteron) [11]. Solid lines: BUU calculations for lead [19].

Both pictures demonstrate the expected behavior. Pions with momenta large enough to excite the Δ resonance ($p_\pi > 227$ MeV), are strongly absorbed ($\alpha \approx 2/3$). The absorption probability decreases fast for smaller momenta and the nuclei are almost transparent for pions with momenta around 100 MeV/c. The influence of FSI and re-scattering can be traced in detail in the pion momentum distributions for heavy nuclei, which are summarized and compared to the deuteron cross sections and to BUU calculations [11, 19] in fig. 15. The distributions for the deuteron approximate the FSI-free case. They show one peak for single pion production, shifting to higher momenta with increasing incident photon energies, and at incident photon energies above 500 MeV a second structure at smaller momenta, corresponding to double pion production. The qualitative behavior of the spectra for heavier nuclei, reflecting the re-scattering of pions and the momentum dependence of their mean-free path, is reproduced by the BUU calculations.

The influence of FSI on pion and η production from nuclei is schematically illustrated in fig. 16 with the help of the BUU calculations [56] for lead. Shown is the distribution of the original creation points of observed pions and η mesons. Most mesons are emitted from the nuclear surface region at densities $\rho \approx \rho_0/2$, where ρ_0 is the normal nuclear matter density. Pions and η mesons are quite similar

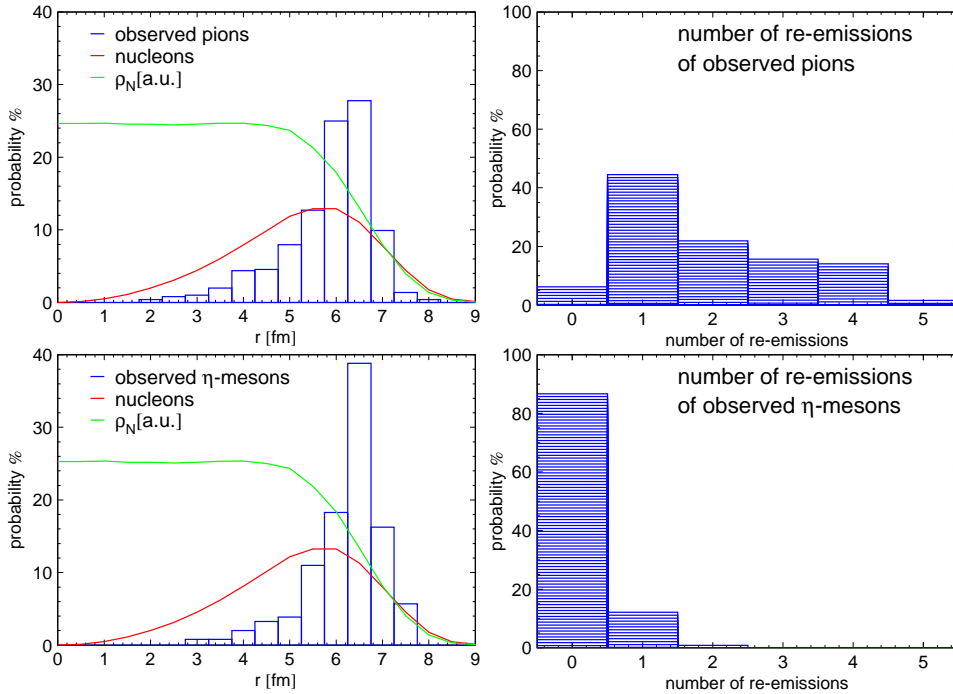


Figure 16: Original creation points (left hand side, histograms) and number of re-absorptions (right hand side) for pions (upper part) and η -mesons which finally leave a lead nucleus [56]. Curves on the right hand side correspond to the distribution of nucleons and the nuclear density.

in this respect. However, they behave very differently as far as the number of re-absorption processes for observed mesons is involved. Pions usually have a long history of propagation through Δ resonance formation, while the observed η mesons are practically undisturbed. The reason is, that re-absorbed η mesons are almost always lost since the S_{11} resonance has a 50% decay branching ratio into $N\pi$.

Although FSI has a large influence on the observed pion spectra, it can not alone explain the disappearance of the second resonance bump. This can be demonstrated with a comparison of the data to BUU calculations. The left hand side of fig. 17 shows the excitation function for inclusive π^0 photoproduction from ^{40}Ca . BUU model calculations which only include all the FSI and the in-medium properties of the Δ produce a much larger bump in the second resonance region as is observed in experiment. Only a substantial broadening of the D_{13} resonance brings the model results closer to the data. The immediate question is, how this result can be re-concealed with the observation that the width of the measured structure for the D_{13} resonance, as shown in fig. 13 for single π^0 photoproduction, is basically identical for heavy nuclei and the (quasi)free nucleon. Lehr and Mosel [55] have argued, that this could be due to a ‘sampling’ effect, which has nothing to do with FSI. The problem is the following: assume that the resonance is broadened due to modified or additional decay channels like e.g. $NN^* \rightarrow NN$ (collisional broadening) in a density dependent way $\Gamma_{coll} = \Gamma_{coll}^o \times \rho/\rho_o$. In that case the branching ratio b_1 of the resonance into any other decay channel with a density independent partial width Γ_1 becomes density dependent since the total width is density dependent. In the simple case with only one open decay channel and the additional in-medium collisional width we have:

$$b_1 = \frac{\Gamma_1}{\Gamma_1 + \Gamma_{coll}^o \times \rho/\rho_o} \quad (5)$$

This means that the branching ratio decreases with increasing density. Since an experiment always integrates over the density distribution, the exclusive reaction channel is dominated by the low density region with the unmodified resonance. In this way, the resonance does not appear broadened but only depleted in strength. This is demonstrated in fig. 17 (right hand side) with a BUU calculation of the D_{13} line shape in single π^0 production [55].

The effect discussed above will of course not occur for a decay channel which is responsible for the broadening, since then the branching ratio will rise as function of the density. This makes it very interesting to study double pion production in the second resonance region. The analysis of double pion

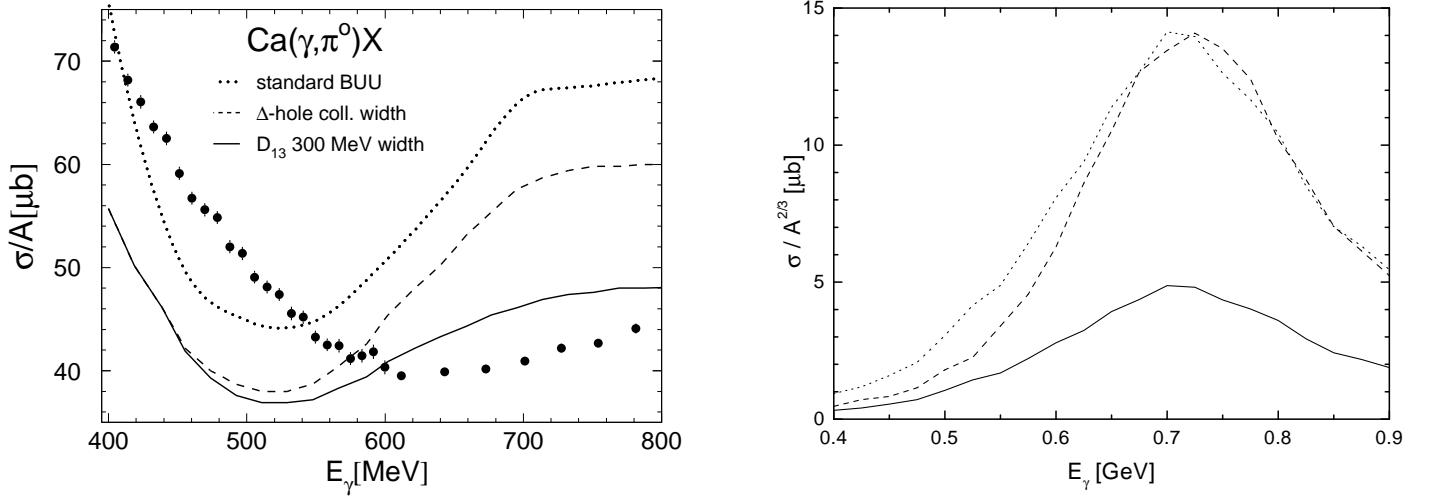


Figure 17: Left hand side: total inclusive π^0 cross section compared to BUU model calculations [53, 19]. Right hand side: prediction for the shape of the D_{13} observed in single π^0 photoproduction. Dashed curve: no in-medium broadening, full curve: 300 MeV in-medium broadening, dotted curve: full curve scaled up by factor 2.9 [55].

production from the free nucleon has shown that a significant contribution to the decay strength of the D_{13} resonance [57, 58] comes from the $D_{13} \rightarrow N\rho$ decay. The large broadening of the D_{13} in-matter spectral function predicted in [8] is related to this channel. In double pion production the ρ contributes to the $\pi^0\pi^\pm$ and $\pi^+\pi^-$ final states, but not to $\pi^0\pi^0$ since $\rho^0 \rightarrow \pi^0\pi^0$ is forbidden. This means, that a possible broadening in the observable excitation functions would be suppressed in $\pi^0\pi^0$ with respect to $\pi^0\pi^\pm$. The measured excitation functions for $\pi^0\pi^0$ and $\pi^0\pi^\pm$ from heavy nuclei are compared to the respective nucleon cross sections in fig. 18. The behavior is identical in both cases, the nuclear cross

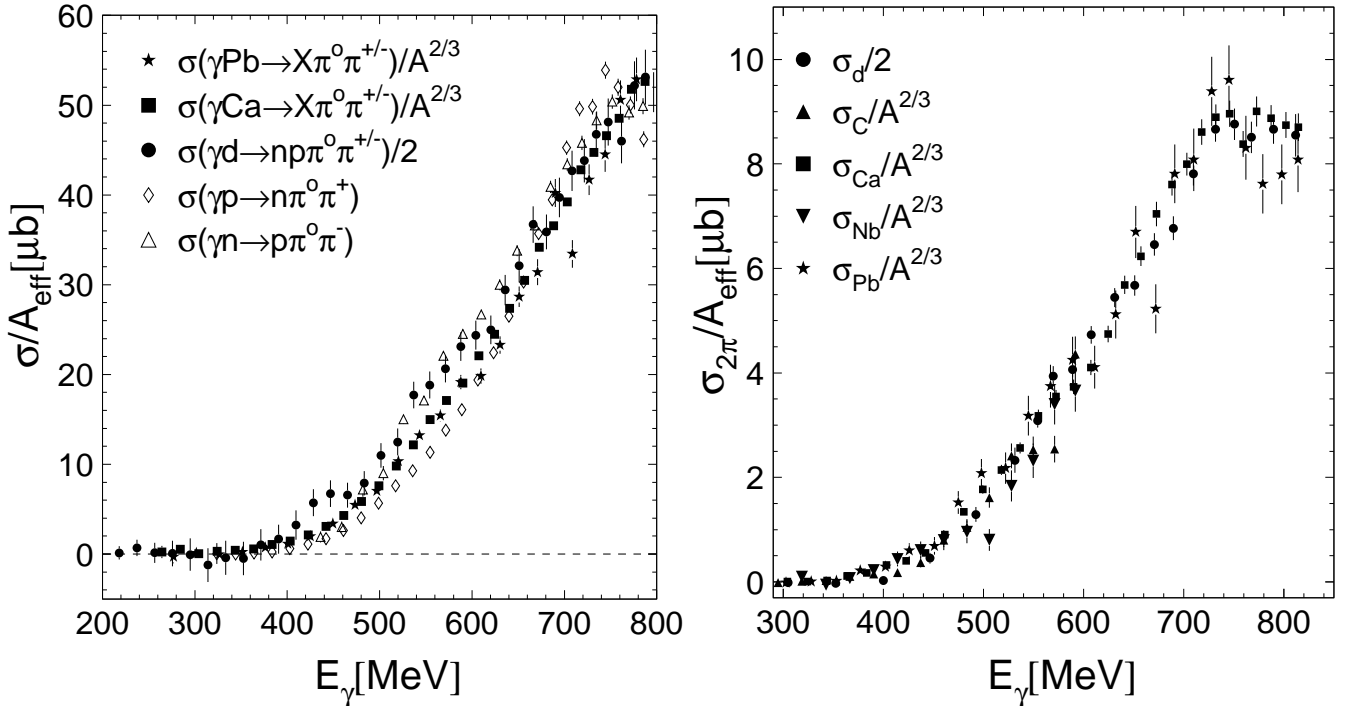


Figure 18: Double pion production from the (quasi)free nucleon and from heavy nuclei. Left hand side: final states $\pi^0\pi^\pm$ [60, 58, 11], right hand side: final state $\pi^0\pi^0$ [59, 11]

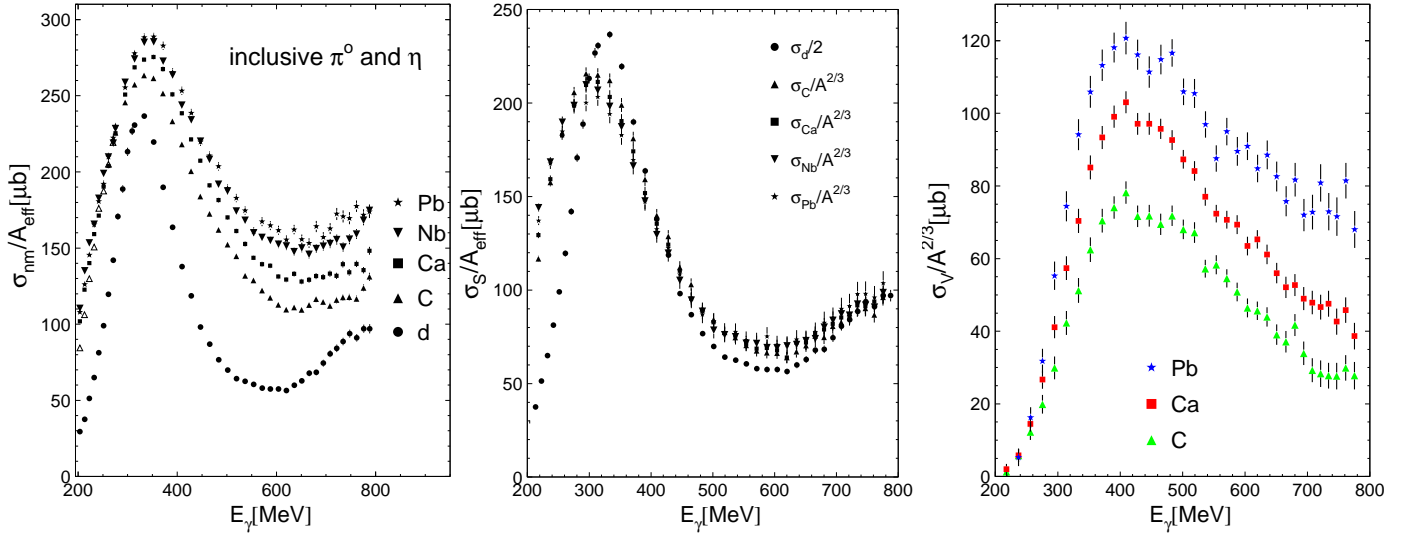


Figure 19: Left hand side: total inclusive cross section σ_{nm} for neutral meson production ($A_{eff}=2$ for the deuteron and $A_{eff} = A^{2/3}$ for $A > 2$), middle: sum of exclusive quasifree and coherent channels σ_S , right hand side: non-quasifree components σ_V .

sections scale with respect to the deuteron following the empirical scaling law:

$$\frac{\sigma_x^{qf}(A)}{A^{2/3}} \approx \frac{\sigma_x^{qf}(d)}{2} \quad (6)$$

which holds also for single π^0 and η photoproduction in this energy region [11]. Consequently, there is no evidence for the predicted broadening of the D_{13} due to the coupling to the ρ meson. The scaling law of course indicates strong FSI, so that the observed cross sections again reflect only the conditions in the low density surface region.

The same is true for the cross section sum σ_S of all quasifree reaction channels with neutral mesons [61]:

$$\sigma_S = \sigma_{\pi^0}^{qf} + \sigma_{\eta}^{qf} + \sigma_{2\pi^0}^{qf} + \sigma_{\pi^0\pi^\pm}^{qf} \quad (7)$$

which is shown in fig. 19 (middle part). Contributions from coherent single π^0 production are included into $\sigma_{\pi^0}^{qf}$ [11] and thus also into σ_S . The behavior of σ_S throughout the second resonance is very similar for the deuteron and the heavy nuclei. The resonance structure is almost identical, no in-medium effects are visible, and the scaling indicates the dominance of FSI effects.

The total inclusive cross section of neutral pion and η photoproduction σ_{nm} (see fig. 19, left hand side) was also extracted in [11]. It includes reactions where for example a single neutral pion is observed which does not fulfill the kinematic constraints of quasifree or coherent reactions. These are mainly reactions with strong FSI, e.g. double pion production with one pion re-absorbed in the nucleus. The behavior is somewhere in between total photoabsorption and the quasifree component. The resonance structure is still visible for heavy nuclei, but it is much less pronounced than for the deuteron. The difference $\sigma_V = \sigma_{nm} - \sigma_S$ between the inclusive cross section and the quasifree components (see fig. 19, right hand side) has a completely different energy dependence. This part of neutral meson production from nuclei does not show any indication of the second resonance bump.

The mass number scaling of the different components of the total neutral meson production cross section follow a simple

$$\sigma(A) \propto A^\alpha \quad (8)$$

behavior. The results of the fitted exponent α are summarized in fig. 20 (left hand side). In case of the quasifree component σ_S the exponent α is close to $2/3$ over the whole energy range. This is the

expected behavior of surface dominated meson production. However, α is significantly larger for the non-quasifree components, in the second resonance region it approaches even unity, which indicates that this contribution probes to some extent the nuclear volume. In this case, the appearance of the second resonance peak in σ_S and its complete suppression in σ_V could indicate a strong density dependence of the effect. The qualitative behavior of α as function of photon energy is reproduced by the BUU calculations [19], however in particular for σ_S the absolute values are underestimated.

A detailed comparison of the different meson production components to the BUU model results is shown for ^{40}Ca in fig. 20 (right hand side). The discrepancy for σ_S at low incident photon energies can be attributed to coherent π^0 photoproduction which is not included in the model. The discrepancy at higher incident photon energies is less well understood, although at least part of it probably comes from two-body absorption processes of the photon of the type $\gamma NN \rightarrow N\Delta$, which are also not included in the BUU model. The strength of the second resonance bump is more or less reproduced for the quasifree part σ_S , but is still significantly overestimated for σ_V , although the calculation already includes the strong broadening of the D_{13} resonance. In summary, there seems to be evidence that the peak structure in the second resonance region is unmodified in the low density nuclear surface region but strongly suppressed in photoproduction reactions which are not entirely dominated by the nuclear surface. A quantitative understanding of this effect is not yet available.

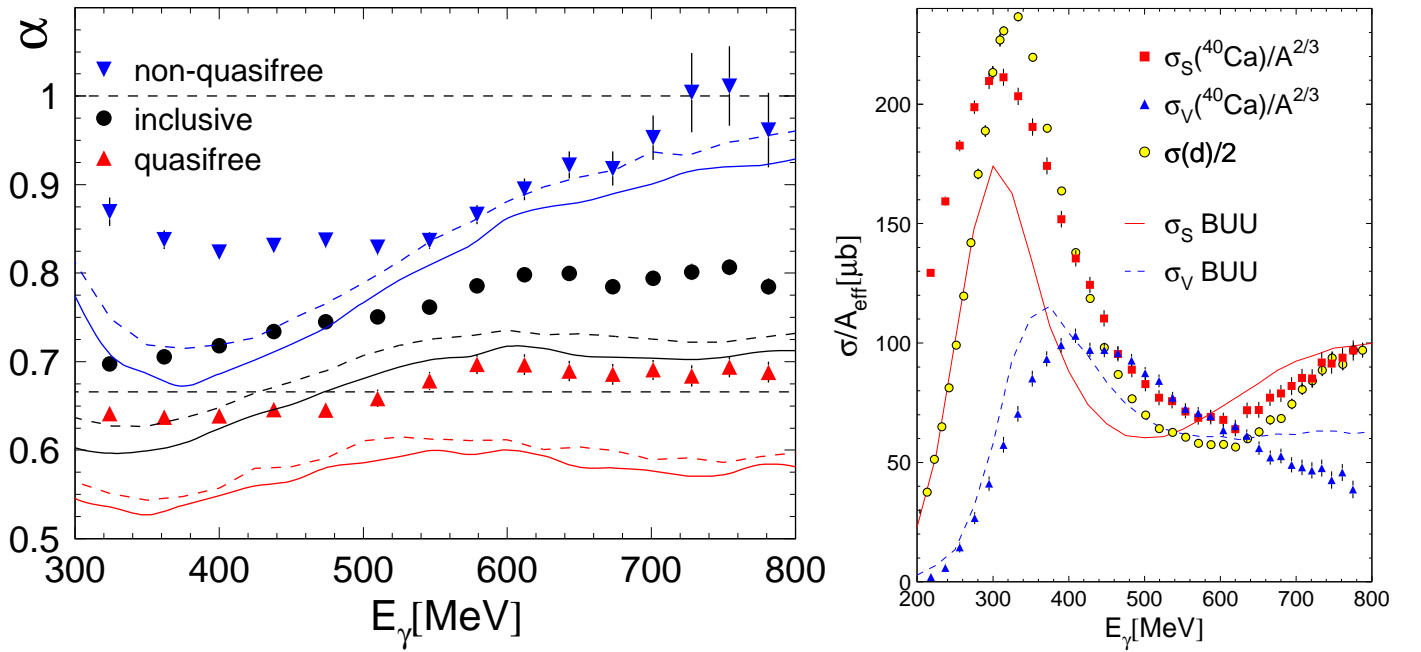


Figure 20: Left hand side: Scaling of the total cross sections σ_{nm} , σ_S and σ_V with mass number as function of incident photon energy. Curves: BUU-model [11, 19] results with slightly different treatment of the P_{33} in-medium width. Right hand side: comparison of σ_S and σ_V for ^{40}Ca to BUU predictions and the cross section for the deuteron.

3.3 η -mesic nuclei

The study of the interaction of mesons with nucleons and nuclei has largely contributed to our understanding of the strong force. In the case of long-lived mesons like charged pions or kaons, secondary beams can be prepared, which allow the detailed investigation of such interactions. Much less is known for short-lived mesons like the η . Their interaction with nuclei is only accessible in indirect ways for example when the mesons are first produced in the nucleus from the interaction of some incident beam

and then subsequently undergo final state interaction (FSI) in the same nucleus. The interaction of η -mesons with nuclei is of particular interest because the existence of bound η -nucleus systems has been discussed. The pion-nucleon interaction at small pion momenta is weak, so that no bound pion-nucleus states can exist. However, the η -N interaction at small momenta is strongly influenced by the existence of the s-wave nucleon resonance $S_{11}(1535)$, which lies close to the η production threshold and couples strongly to the $N\eta$ -channel [33, 47]. An attractive s-wave interaction was already found in coupled channel analysis of η production by Bhalerao and Liu [62] (η N scattering length: $a=0.27+i0.22$). The first suggestion of bound η -nucleus systems with $A > 10$ termed η -mesic nuclei goes back to Liu and Haider [63]. However, although it was searched in different reactions [64] for such states, up to now no conclusive evidence was reported. Recently, Sokol et al. [65] claimed the formation of η -mesic nuclei with mass number $A = 11$ (carbon, beryllium) in the $\gamma+^{12}\text{C}$ reaction with the decay chain:

$$\gamma + A \rightarrow N_1 + (A - 1)\eta \rightarrow N_1 + (N_2 + \pi) + (A - 2) . \quad (9)$$

More recent analyses of the η N scattering length found larger values of its real part which span the entire range from 0.2 - 1.0 and most cluster between 0.5 - 0.8 (see e.g. [66]). These results prompted speculations about the existence of light η -mesic nuclei, in particular ^2H , ^3H , ^3He , and ^4He (see e.g. [66]). Such states have been sought in experiments investigating the threshold behavior of hadron induced η -production reactions [67], in particular $pp \rightarrow pp\eta$, $np \rightarrow d\eta$, $pd \rightarrow \eta^3\text{He}$, $\vec{d}d \rightarrow \eta^4\text{He}$, and $pd \rightarrow pd\eta$. All reactions show more or less pronounced threshold enhancements. However, so far there is no conclusive evidence that the final state interaction is strong enough to form quasi-bound states.

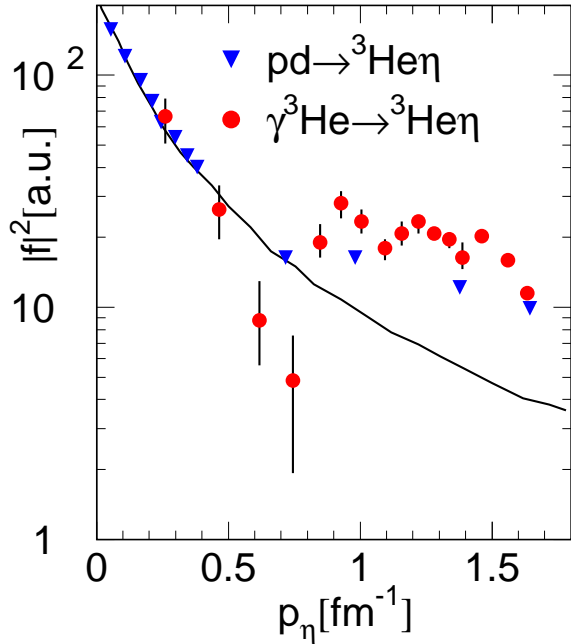


Figure 21: Squared amplitudes for proton [67] and photon [12] induced η production (arb. normalized) on ^3He . Solid curve: optical model fit to threshold data [67].

If such states do exist, they should show up as threshold enhancements independently of the initial state of the reaction. Photoproduction of η -mesons from light nuclei was also investigated in detail, in particular with TAPS at MAMI [48, 68, 69, 70, 71, 49, 12] and again, threshold enhancements were observed. These experiments furthermore clearly demonstrated that the reaction is dominated by an isovector, spin-flip amplitude (see e.g. [49]). Consequently, the $I = J = 1/2$ nuclei ^3He and ^3H are the only light nuclei where non-negligible contributions from coherent η -photoproduction, which is the ideal channel for the search of near-threshold quasi-bound states, can be expected. The coherent reaction was indeed clearly identified for ^3He [12], and after reduction of the different phase space factors, it shows a threshold behavior which is very similar to the $pd \rightarrow ^3\text{He}\eta$ reaction (see fig. 21). Since the ^3He recoil nuclei do not reach the detectors, the identification must rely on the different reaction kinematics for coherent (final state $\eta+^3\text{He}$) and breakup (final states $\eta + pd$ or $\eta + ppn$) photoproduction. For this purpose missing energy spectra for the η mesons were constructed under the assumption of coherent kinematics [12].

In these spectra contributions from coherent production peak around zero while contributions from the breakup reactions where the recoil is mainly taken by one participant nucleon are shifted to negative values. Typical spectra for the most interesting low energy region are summarized in fig. 22.

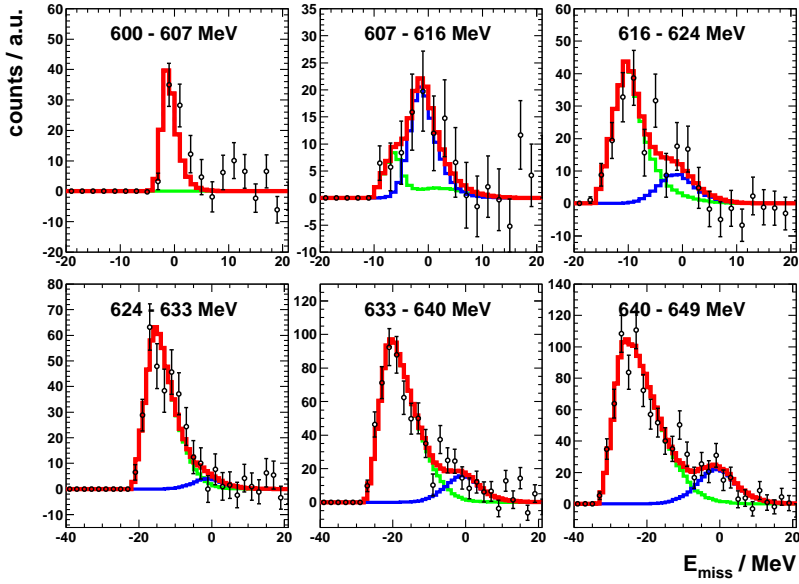


Figure 22: Missing energy spectra assuming coherent reaction kinematics for different ranges of incident photon energy. The simulated shapes for the coherent (black histograms) and breakup (light grey histograms) parts are fitted to the data. The dark grey histograms correspond to the sum of both.

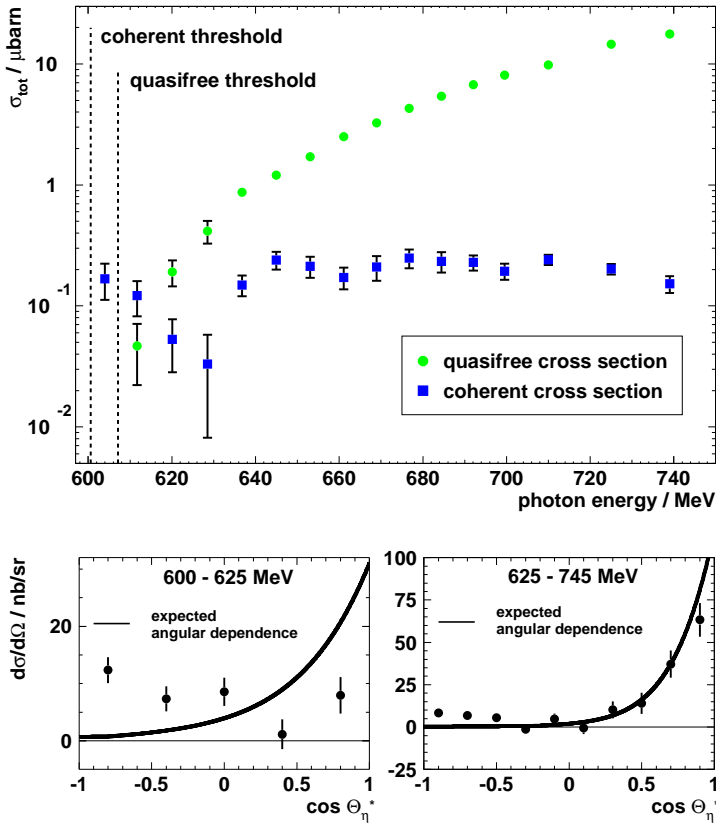


Figure 23: Upper part: total cross section for quasifree and coherent η production. Lower part: angular distributions for ${}^3\text{He}(\gamma, \eta){}^3\text{He}$. Solid curves: angular dependence from ${}^3\text{He}$ form factor.

Such pion - nucleon pairs have been searched for in the channel $\pi^0 - p$, which is best suited for the TAPS detector. Their excitation function is shown in fig. 25. Background was estimated by a comparison of the yields for back-to-back production (opening angles larger than 170°) to the yield at opening angles $150 - 170^\circ$. The back-to-back emission shows a structure at the production threshold for η -mesons (600 MeV), which is particularly visible in the difference of the two excitation functions (see fig. 25, right hand side).

The threshold behavior of the coherent photon induced reaction (see fig. 23) is remarkable. In contrary to the breakup process it does not smoothly approach the threshold but shows a peak-like structure. Furthermore, the angular distribution in vicinity of the threshold does not follow the behavior expected from the ${}^3\text{He}$ form factor but seems to be much more isotropic. Both could be indications for the formation of an intermediate quasi-bound state.

When an η mesic nucleus is formed, the η meson can be absorbed on a nucleon which is excited into the $S_{11}(1535)$ resonance which can subsequently decay via pion emission (50% branching ratio) (see fig. 24). When the state is populated at incident photon energies below the coherent η production threshold this is basically the only possible decay mode of the system (the electromagnetic decay of the η meson itself is much slower). At energies above the coherent threshold this channel competes with the emission of η mesons. The signature of the additional decay channel are pion - nucleon pairs which are emitted back-to-back in the rest frame of the η mesic nucleus.

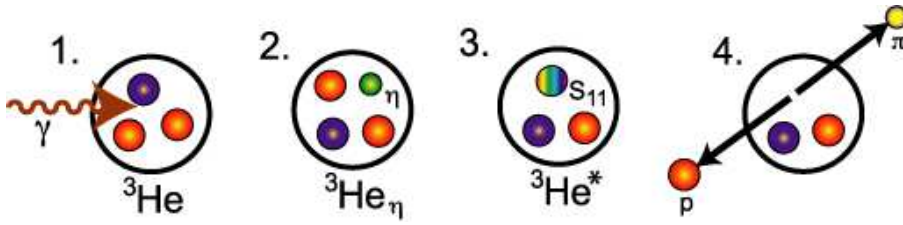


Figure 24: Formation of an η mesic nucleus and its decay via emission of back-to-back nucleon-pion pairs.

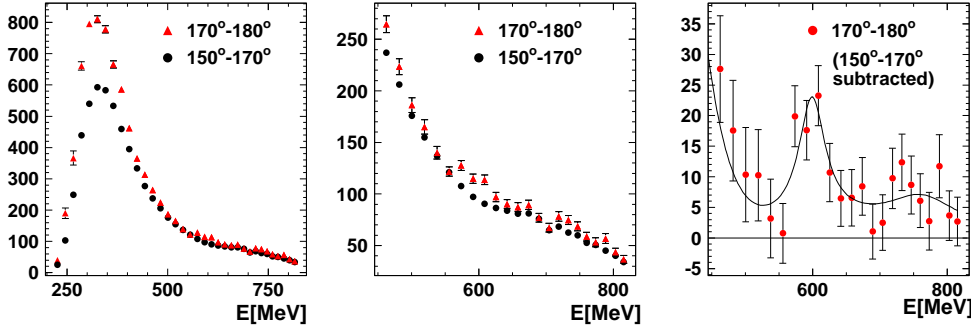


Figure 25: Left and center: excitation functions for the $\pi^0 - p$ final state. Triangles: opening angles between $170 - 180^\circ$, dots: $150 - 170^\circ$ in the incident photon - ^3He cm system. Right: difference of both distributions fitted with a Breit-Wigner curve.

It was analyzed [12], if the observed effect in coherent η production and the structure in the excitation function of pion-nucleon emission are roughly consistent with the hypothesis that both are different decay channels of an η mesic nucleus. The η - mesic (quasi)bound state was parameterized with a Breit-Wigner curve at position W with width Γ . Proper phase space factors and the energy dependent branching ratio of the S_{11} resonance have been taken into account [12]. The result of the fit of this simplified model is shown in fig. 26. A consistent description of the cross sections for both decay channels is possible for the following parameters of the Breit-Wigner resonance: $W = (1481 \pm 4)$ MeV, $\Gamma = (25 \pm 6)$ MeV. This corresponds to a (quasi)bound state of a width of ≈ 25 MeV, which is ‘bound’ by (4 ± 4) MeV.

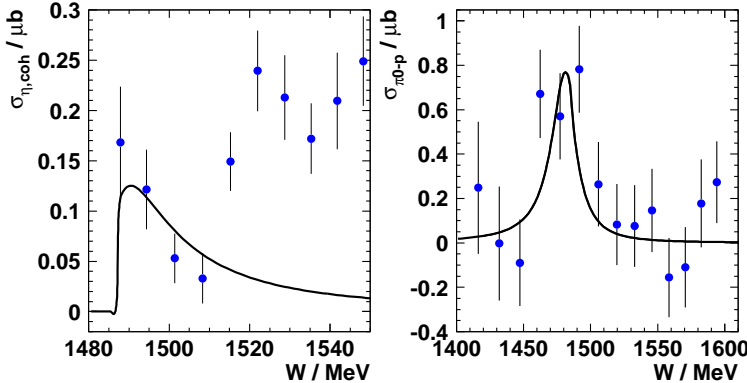


Figure 26: Comparison of the two possible decay channels. Left: coherent η channel. Solid curves: best common fit. Right: background subtracted excitation function of pion-nucleon back-to-back pairs.

Acknowledgments

The discussed results are part of the experimental program of the TAPS collaboration. I like to acknowledge in particular the contributions of M. Pfeiffer (eta-mesic nuclei) and F. Bloch, S. Janssen, M. Röbig-Landau (heavy nuclei). This work was supported by the Swiss National Fund and the DFG.

References

- [1] M. Lutz, S. Klimt, and W. Weise, *Nucl. Phys. A* 542 (1992) 521
- [2] G.E. Brown and M. Rho, *Phys. Rev. Lett.* 66 (1991) 2720
- [3] T. Hatsuda, T. Kunihiro, and H. Shimizu, *Phys. Rev. Lett.* 82 (1999) 2840
- [4] G. Agakichiev et al., *Phys. Rev. Lett.* 75 (1995) 1272
- [5] D. Adamova et al., *Phys. Rev. Lett.* 91 (2003) 042301
- [6] F. Bonutti et al., *Phys. Rev. Lett.* 77 (1996) 603
- [7] A. Starostin et al., *Phys. Rev. Lett.* 85 (2000) 5539
- [8] M. Post, J. Lehr, and U. Mosel, *Nucl. Phys. A* 741 (2004) 81
- [9] M. Rößig-Landau et al., *Phys. Lett. B* 373 (1996) 45
- [10] B. Krusche et al., *Eur. Phys. J. A* 6 (1999) 309
- [11] B. Krusche et al., *Eur. Phys. J. A* 22 (2004) 277
- [12] M. Pfeiffer et al., *Phys. Rev. Lett.* 92 (2004) 252001
- [13] J.G. Messchendorp et al., *Phys. Rev. Lett.* 89 (2002) 222302
- [14] R. Novotny, *IEEE Trans. on Nucl. Science* 38 (1991) 379
- [15] A.R. Gabler et al., *Nucl. Instr. Meth. A* 346 (1994) 168
- [16] M. Fuchs et al., *Phys. Lett. B* 368 (1996) 20
- [17] K. Büchler et al., *Nucl. Phys. A* 570 (1994) 580
- [18] D. Drechsel, O. Hanstein, S.S. Kamalov, and L. Tiator, *Nucl. Phys. A* 645 (1999) 145
- [19] J. Lehr, M. Effenberger, and U. Mosel, *Nucl. Phys. A* 671 (2000) 503
- [20] B. Krusche et al., *Phys. Lett. B* 526 (2002) 287
- [21] D. Drechsel, L. Tiator, S.S. Kamalov, and S.N. Yang, *Nucl. Phys. A* 660 (1999) 423
- [22] J. Arends et al., *Z. Phys. A* 311 (1983) 367
- [23] W. Cassing, V. Metag, U. Mosel, and K. Niita, *Phys. Rep.* 188 (1990) 363
- [24] F. Lenz and E.J. Moniz, *Com. Nucl. Part. Phys.* 9 (1980) 101
- [25] J.H. Koch, E.J. Moniz, and N. Ohtsuka, *Ann. Phys.* 154 (1984) 99
- [26] M. Hirata et al., *Ann. Phys.* 120 (1979) 205
- [27] U. Siodlaczek et al., *Eur. Phys. J. A* 10 (2001) 365
- [28] F. Rambo et al., *Nucl. Phys. A* 660 (2000) 69
- [29] Th. Frommhold et al., *Phys. Lett. B* 295 (1992) 28
- [30] N. Bianchi et al., *Phys. Lett. B* 299 (1993) 219
- [31] N. Bianchi et al., *Phys. Lett. B* 325 (1994) 333
- [32] A. Braghieri et al., *Phys. Lett. B* 363 (1995) 46
- [33] B. Krusche et al., *Phys. Rev. Lett.* 74 (1995) 3736
- [34] M. MacCormick et al., *Phys. Rev. C* 53 (1996) 41
- [35] F. Härter et al., *Phys. Lett. B* 401 (1997) 229
- [36] M. Wolf et al., *Eur. Phys. J. A* 9 (2000) 5
- [37] F. Renard et al., *Phys. Lett. B* 528 (2002) 215
- [38] M. Dugger et al., *Phys. Rev. Lett.* 89 (2002) 222002
- [39] V. Crede et al., [hep-ex/0311045](https://arxiv.org/abs/hep-ex/0311045)

- [40] W.T. Ciang et al., *Nucl. Phys. A* 700 (2002) 327
- [41] O. Bartholomy et al., *hep-ex/0407022*
- [42] L.A. Kondratyuk et al., *Nucl. Phys. A* 579 (1994) 453
- [43] W.M. Alberico et al., *Phys. Lett. B* 321 (1994) 177
- [44] J.A. Gomez Tejedor and E. Oset, *Nucl. Phys. A* 600 (1996) 413
- [45] M. Hirata, K. Ochi, T. Takaki, *Phys. Rev. Lett.* 80 (1998) 5068
- [46] B. Krusche and S. Schadmand, *Prog. in Part. and Nucl. Phys.* 51 399 2003
- [47] B. Krusche et al., *Phys. Lett. B* 397 (1997) 171
- [48] B. Krusche et al., *Phys. Lett. B* 358 (1995) 40
- [49] J. Weiss et al., *Eur. Phys. J. A* 16 (2003) 275
- [50] T. Yorita et al. *Phys. Lett. B* 476 (200) 226
- [51] H. Yamazaki et al., *Nucl. Phys. A* 670 (2000) 202c
- [52] J. Lehr, M. Post and U. Mosel, *Phys. Rev. C* 68 (2003) 044601
- [53] B. Krusche et al., *Phys. Rev. Lett.* 86 (2001) 4764
- [54] R.C. Carrasco, *Phys. Rev. C* 48 (1993) 2333
- [55] J. Lehr and U. Mosel, *Phys. Rev. C* 64 (2001) 042202
- [56] A. Hombach et al., *ZPA* 352 (1995) 223
- [57] A. Zabrodin et al., *Phys. Rev. C* 60 (1999) 055202
- [58] W. Langgärtner et al., *Phys. Rev. Lett.* 87 (2001) 052001
- [59] V. Kleber et al., *Eur. Phys. J. A* 9 (2000) 1
- [60] A. Zabrodin et al., *Phys. Rev. C* 55 (1997) R1617
- [61] B. Krusche et al., *Eur. Phys. J. A*, *accepted* (2004) ; nucl-ex/0411009
- [62] R.S.Bhalerao and L.C.Liu, *Phys. Rev. Lett.* 54 (1985) 865
- [63] L.C.Liu and Q.Haider, *Phys. Rev. C* 34 (1986) 1845
- [64] R.E.Chrien et al., *Phys. Lett. B* 60 (1988) 2595 ; J.D.Johnson et al., *Phys. Rev. C* 47 (1993) 2571
- [65] G.A. Sokol et al., *nucl-ex/0011005; nucl-ex/0106005*
- [66] T.Ueda, *Phys. Rev. Lett.* 66 (1991) 297 ; T.Ueda, *Phys. Lett. B* 291 (1992) 228 ; C.Wilkin, *Phys. Rev. C* 47 (1993) R938 ; S.A.Rakityanski et al., *Phys. Lett. B* 359 (1995) 33 ; S.A. Rakityanski et al., *Phys. Rev. C* 53 (1996) R2043 ; A.M. Green and S. Wycech, *Phys. Rev. C* 54 (1996) 1970 ; A.M. Green and S. Wycech, *Phys. Rev. C* 55 (1997) R2167 ; N.N. Scoccola, D.O. Riska, *Phys. Lett. B* 444 (1998) 21 ; A.M. Green and S. Wycech, *Phys. Rev. C* 60 (1999) 35208 ; N.V. Shevchenko et al., *Eur. Phys. J. A* 9 (2000) 143 ; V. Yu. Grishina et al., *Phys. Lett. B* 475 (2000) 9 ; H. Garcilazo and M.T. Pena, *Phys. Rev. C* 63 (2001) R21001 ; A. Sibirtsev et al., *Phys. Rev. C* 65 (2002) 044007
- [67] H. Calén et al., *Phys. Lett. B* 366 (1996) 39 ; F. Plouin et al., *Phys. Rev. Lett.* 65 (1990) 690 ; H. Calén et al., *Phys. Rev. Lett.* 80 (1998) 2069 ; B. Mayer et al., *Phys. Rev. C* 53 (1996) 2068 ; N. Willis et al., *Phys. Lett. B* 406 (1997) 14 ; F. Hibou et al., *Eur. Phys. J. A* 7 (2000) 537 ; R. Bilger et al., *Phys. Rev. C* 65 (2002) 044608
- [68] P. Hoffmann-Rothe et al., *Phys. Rev. Lett.* 78 (1997) 4697
- [69] V. Hejny et al., *Eur. Phys. J. A* 6 (1999) 83
- [70] J. Weiss et al., *Eur. Phys. J. A* 11 (2001) 371
- [71] V. Hejny et al., *Eur. Phys. J. A* 13 (2002) 493
- [72] A. Sibirtsev et al., *nucl-th/0407073; C. Hanhart, hep-ph/0408204*
- [73] B. Krusche et al., *experiment proposal MAMI A2/7-03*